RSC Advances

PAPER

View Article Online
View Journal | View Issue

Cite this: *RSC Adv.*, 2023, **13**, 4340

Thermal plasma processing of *Moringa oleifera* biochars: adsorbents for fluoride removal from water†

Moumita Gourai,[a] Ashok K. Nayak,[ab] Partha S. Nial,[ab] Bijaylaxmi Satpathy,[c] Rajashree Bhuyan,[a] Saroj K. Singh[ab] and Umakanta Subudhi *[ab]

Anthropogenic activities accelerate fluoride contamination in groundwater, which largely affects public health. Though biochars have been explored for defluoridation, the plasma technology-based production of biochars has not received as considerable attention as other methods and it is also important that biochars be tested on groundwater samples. In the present study, for the first time, we report the preparation of biochars from different parts of *Moringa oleifera* using thermal plasma processing and demonstrate fluoride adsorption in both synthetic and contaminated groundwater. Water samples were collected from different locations in Nuapada district of Odisha such as Kotamal-Makardampada (20°24′46″N 82°37′19″E), Pandrapathar (20°34′41″N 82°39′25″E), Karlakot-Kadobhata (20° 22′52″N 82°37′24″E), Kotamal-Jhakarpada (20°24′35″N 82°37′20″E), and Dohelpada (20°33′50″N 82° 38′57″E). The *Moringa* leaf samples are processed at 1600 °C for 3 min in an inert atmosphere under a continuous flow of argon to get suitable biochars. The plasma-synthesized biochars contain larger exposed surfaces, which are efficient for the adsorption of fluoride. The prepared biochars were highly porous, amorphous, and contain > 72% carbon, which increases the efficiency of defluoridation due to the surface adsorbate site exposed. XRD of the samples showed the presence of calcium hydroxide, magnesium oxide, and calcium oxide, and large peaks of carbon. Raman data showed the double bond of carbon with oxygen in the form of carbonyl bonds, thioether, and sulfhydryl bonds, which contribute to the protonated site for the adsorption of fluoride, and assist in water penetration and swelling of biochars. The biochar of *Moringa oleifera* is very efficient for the adsorption of fluoride from standard samples as well as groundwater samples up to a concentration of 6 ppm. Conclusively, the present investigation shows that *Moringa oleifera* leaves are a good alternative adsorbent that could be used for the removal of fluoride from groundwater samples with > 85% removal in 18 h using 1 g biochar for 100 mL or 10 g biochar for 1 L water containing 4 ppm fluoride. To our knowledge, this is the first report on the thermal plasma-based production of *Moringa* biochars for the removal of fluoride from drinking water.

Received 25th November 2022
Accepted 9th January 2023

DOI: 10.1039/d2ra07514h

rsc.li/rsc-advances

1. Introduction

Fluoride is most frequently found in ground water and has become one of the most serious environmental hazards globally. Nevertheless, groundwater is the main source of drinking water in rural areas and few ground water sources in rural Indian villages have been found to be contaminated with fluoride in recent times.[1,2] Naturally, the ground water in India contains fluoride due to the geological distribution, *i.e.*, presence of fluoride belt-3 across the country.[3] Additionally, due to anthropogenic activities, the toxic level of fluoride in groundwater has become an urgent scientific problem that has to be solved in the interest of public health.[4,5] Fluoride enters the body mostly through fluoride-containing drinking water, which is contaminated by the industrial effluent from food, cosmetic, and drug industries. Moreover, the presence of fluoride in drinking water has high affinity for calcium phosphate in bones, which is incorporated into the crystal lattice.[6] Nevertheless, fluoride is known to cross the cell membrane and enter soft tissues. Though the maximum safe limit of fluoride prescribed by WHO is 1.5 mg L^{-1},[6,7] nearly 200 000 people are in risk in Nuapada and Kalahandi districts of Odisha because of objectionable fluoride contents in the range of 3.88 to

[a]*Biochemistry & Biophysics Laboratory, CSIR-Institute of Minerals & Materials Technology, Bhubaneswar 751 013, Odisha, India. E-mail: usubudhi@immt.res.in; subudhisai@gmail.com*

[b]*Academy of Scientific & Innovative Research (AcSIR), Ghaziabad 201002, Uttar Pradesh, India*

[c]*Rural Water Supply and Sanitation Department, Nuapada District 766105, Odisha, India*

† Electronic supplementary information (ESI) available. See DOI: https://doi.org/10.1039/d2ra07514h

5.95 mg L^{-1}.[8] Dental, skeletal fluorosis, and crippling disorder are also noticed among people in the district of Nuapada.[9] Since no therapeutics is available for fluorosis, preventive healthcare measures of this disease are the urge of the society. Exposure to fluoride has a number of adverse effects on human health including crippling skeletal fluorosis, which is a significant cause of morbidity.[6] The effect of excess of fluoride in human body causes mottled enamel at 2 ppm, osteoporosis at 5 ppm, osteosclerosis at 8 ppm, crippling fluorosis at 20–80 ppm, mental retardation at 100 ppm, and kidney failure at 125 ppm.[8] Thus, the acceptable limit for fluoride in groundwater water is set to be 0.5–1.5 ppm. However, over 200 million people in the world are affected by a fluoride concentration > 1.5 ppm in drinking water.

Although many methods such as electrocoagulation, ion-exchange, and adsorption are available for fluoride removal,[10–13] adsorption is the preferred method, because of the simple and economic process, and a lot of natural adsorbents are available. The removal of pollutants from aqueous environments *via* adsorption onto a microporous active carbon surface is a sustainable method because of the high adsorption capacity. The purification method, physical, chemical or biological, is based on the load of contaminants. The biosorption technique is suitable for lower contaminant doses, while the physical and chemical techniques are suitable for medium to high contaminant doses.[14,15] The activation process involves heating the charcoal to remove substances that have adhered to it as well as to break it down into finer particles and thus increase the surface area. Activated carbon has been used for its adsorptive properties as a 'universal antidote' in cases of poisonings, filter-aid agents, and decolorization processes.[16] Activated carbon is a microporous adsorbent that can be produced from a variety of carbonaceous materials including oak wood,[17] bamboo,[18,19] coconut buttons,[20] okra waste,[21] maize cobs,[22] cocoa shells,[23] chitin[24], pine wood,[25] sawdust,[26] and seed hull.[27] Thus, activated carbons can be potential adsorbents for various contaminants including metal ions.[28]

Porous carbon is an excellent adsorbent for the removal of fluoride as it has a large surface area-to-volume ratio, hence a large surface for the adsorption of fluoride.[29] The larger the surface area, the more will be the adsorption and the more will be the removal. Activated carbon is derived by grinding charcoal into smaller particles. Charcoal is used in raw and activated states for the removal of heavy metals and toxic contaminants from aqueous solutions.[30,31] Most of the sources are agricultural wastes which are formed as by-products of agricultural practices. Activated carbons are commonly characterized by the mode of activation. Unique adsorption properties of activated carbon are due to high surface area, microporosity, and a broad range of surface functional groups.[29] The structure of activated carbon is composed of carbon atoms that are arranged in parallel stacks of hexagonal layers, exclusively cross-linked and tetrahedrally bonded. Several heteroatoms including oxygen, hydrogen, and nitrogen are detected in the carbon matrix, in the form of single atoms and functional groups. Oxygen is the dominant heteroatom in the carbon matrix, while functional groups such as carbonyl, carboxyl, phenol, enols, lactones, thioether, and carbamoyl have been observed in the activated carbon.[32] Nevertheless, such unique functional groups sometimes available in noble bio adsorbents or biochars are prepared based on an advanced technique like thermal plasma processing. Herein, for the first time, we report the synthesis of biochars from *Moringa oleifera via* thermal plasma processing for adsorption of fluoride.

The serious problem of fluorosis is creating havoc in few districts of Odisha and is considered as a serious health hazard, which demands economic and sustainable techniques for the defluorination of contaminated ground water. Various low-cost materials have been developed in the recent past and used for the removal of fluoride from aqueous solutions.[33] Though biochars are explored for the removal of metal ions such as chromium from drinking water,[34,35] no attempt has been made for the removal of fluoride. *Moringa* plant is chosen for the preparation of biochars as it is widely available in India, and withstands long period of drought, grows well in arid and semi-arid regions, and also tolerates soil with a pH between 4.5 and 8. Thus, such adaptable species that grows faster is suitable for biochar production.[36] Since 18th Century BC, *Moringa oleifera* has been used as medicine in India and recognised in the Ayurvedic and Unani systems of medicine. The medicinal properties include pharmacological, antimicrobial, anti-diabetic, anticarcinogenic, anti-inflammatory, antioxidant, cardioprotective, and hepatoprotective uses.[37] Keeping this as background, different parts of *Moringa oleifera* have been processed using a thermal plasma reactor and the produced biochar was thoroughly characterized using various biophysical techniques. Finally, the leaf biochar of this plant was used as a potential material for defluoridation of drinking water and also tested for antibacterial activity. To our knowledge, this is the first report on the production of *Moringa* biochars *via* thermal plasma processing and their application for fluoride removal and as antibacterial agents.

2. Materials and methods

2.1 Collection of raw materials and pre-processing for biochars

For the current study, ground water samples contaminated with fluoride were obtained from different locations in Nuapada district of Odisha such as Kotamal-Makardampada (20°25′45″N 82°39′6″E), Pandrapathar (20°34′41″N 82°39′25″E), Karlakot-Kadobhata (20°22′52″N 82°37′24″E), Kotamal-Jhakarpada (20° 25′48″N 82°39′8″E), and Dohelpada (20°33′50″N 82°38′57″E) (Table S1†). Biological samples from parts such as the leaf, bark, stem, and seeds of *Moringa oleifera* were collected from the kitchen garden of Dr Umakanta Subudhi. Samples were thoroughly washed with Milli-Q (MQ) water to remove dust and other impurities. The materials were initially air dried separately, followed by drying in an oven at 80 °C for 2 to 3 h and then fed into a thermal plasma reactor. Biochars were used without any chemical treatment or grinding to reduce the cost. All other chemicals used in the experiments were of analytical grade.

2.2 Preparation of biochars using thermal plasma reactor

The partially dried samples of *Moringa* were processed in a graphite crucible and the extended arc was formed by the movement of the top graphite electrode with an axial hole through which the argon plasma forming gas was introduced.[38] The samples were separately carbonized at 1600 °C for 3 min in the presence of argon gas, which provided an inert environment. The experiments were carried out in batch operations and experimental conditions such as power and time were constant. Typical material processing conditions such as argon gas flow at 2 L min^{-1}, a current of 300 A, a load voltage of 50 V, and a temperature of 1600 °C were maintained throughout the experiments.[38] After 3 min, argon gas was allowed to flow for few more minutes till the crucible cools down to room temperature to maintain the oxygen-deficient condition. During carbonization and activation processes, volatile materials were released as gas and liquid products and left with high carbon content materials.[38] Biochars were generated in triplicate for each experimental condition. The prepared biochars were directly used for the adsorption study without further modification and treatment.

2.3 Biochars prepared from different parts of moringa

Different parts of *Moringa oleifera* such as the drum stick, bark-free oldest stem, bark-free older stem, bark-free younger stem, bark, leaf, younger stem, younger stem with leaf and seed were dried separately and taken for plasma processing at 1600 °C, and thus, the biochars collected were used separately for fluoride removal from 2 ppm standard samples for 12 h. During carbonization and activation processes, organic substances become unstable as a result of the heat causing the molecules to break their bonds and linkages. During activation steps, volatile materials were released as gas and liquid products, which evaporate off leaving a material with a high carbon content.[39]

2.4 Biochar-based fluoride adsorption in synthetic water

Batch adsorption experiments were conducted to investigate the effect of pH, adsorbent dosage, size of adsorbent and contact time. All the experiments were conducted at 25 °C. The standard fluoride solution was prepared from 100 ppm NaF stock. Primarily, a 2 ppm fluoride-containing standard solution was exposed to different amounts of biochars, namely, 0.0125, 0.025, 0.05 and 0.1 g for 12 h. The fluoride content was estimated in the treated sample after the incubation period. Further, experiments were optimized by performing adsorption with 10 mL of synthetic sample containing 2, 4, 8 and 12 ppm fluoride. This range was selected based on the fluoride concentrations found in groundwater in India and other countries. Exactly 0.1 g of biochar was added to the 10 mL solution and, thus, 1 g for 100 mL of synthetic solution followed by agitation for specified times to a maximum of 18 h at room temperature. The contact time and conditions were selected based on preliminary experiments, which demonstrated that equilibrium was established in 18 h. The solutions were then filtered and the absorbance of the samples was recorded at 620 nm. Control samples of 2, 4, 8 and 12 ppm without biochars were made for comparison after adsorption at fixed intervals of studies. A fluoride estimation kit was used for making the standard curve and also for the analysis of fluoride in ground water using manufacturer's instructions.

2.5 Fluoride adsorption in contaminated groundwater using leaf and seed biochars

The seed and leaf biochars were selected for the removal of fluoride from contaminated ground water. Five different ground water samples were collected from the village of Kotamal, Pandrapathar, Karlakot, and Dohelpada belonging to the district of Nuapada, Odisha (Table S1†). Samples 2, 3 and 4 were used for the fluoride adsorption study. However, Samples 1 and 5 have not been processed due to very low and high amounts of F^-. In brief, 0.1 g of biochar was allowed to interact with 10 mL of ground water Samples 2, 3 and 4 and incubated for 18 h at room temperature with intermittent shaking. Water samples were then filtered and the fluoride content was estimated in the treated sample after the incubation period.

2.6 Characterization of biochars using FESEM

The surface morphology and elemental analysis of biochars was performed using a field emission scanning electron microscope model SUPRA GEMINI55 with a resolution of 1.7 nm at 1 kV.[40] The FESEM images of leaf and seed biochars were acquired before adsorption. Similarly, the biochar used for fluoride adsorption was collected and dried for FESEM analysis. The EDX spectra were also analyzed for both seed and leaf biochars to examine the elemental composition.

2.7 X-ray diffraction analysis *of biochars*

For the identification of chemical compounds and their respective phases on the basis of their dissimilar crystalline structure, samples were dried, mounted and dispersed for X-ray diffraction analysis (Model STR 500). A high-voltage field accelerates electrons with very high-speed collides with a metal target and then rapid deceleration of electrons converts its kinetic energy to produce X-ray radiation.[41] The X-ray radiation wavelength at 514 nm laser identifies the phase identification of powder at resolution 2θ: 2° to 100° and in the range of 100–4000 cm^{-1}.

2.8 Antimicrobial property of biochars

For studying the antibacterial activity, 10 mL of autoclaved MQ water was taken into each of the four 50 mL falcon tubes containing 0 g, 0.001 g, 0.01 g and 0.1 g of biochar to achieve 0%, 0.01%, 0.1% and 1% respectively. Then, 100 μL of inoculum containing 2×10^7 cells was added to each tube and the tubes were then transferred to a shaking incubator and kept for 6 h. After 6 h, serial dilution was made up to 10^{-3} and 10^{-4} times for each tube and a spread plate technique was followed in triplicate by taking 50 μL of sample from 10^{-3} and 10^{-4} dilution tubes. The same method was done for each tube except 1% biochar tube, where spreading was done from 10^{-2} and 10^{-3}

dilutions. The plates were kept in an incubator at 37 °C for overnight culture. The following day, the colonies were calculated and CFU mL^{-1} was noted down, as mentioned earlier.[42]

2.9 Statistical analysis

All data are presented as mean ± standard deviation with $n = 3$ or 5. The level of significance was determined by one-way ANOVA followed by Duncan's new multiple range test. A difference was considered statistically significant at $p \leq 0.05$.

3. Results and discussions

3.1 Preparation of biochars using a thermal plasma reactor

Plasma technology is preferred over the conventional pyrolysis process due to high energy density, fast heating and reaction rates, ability to achieve very high temperatures in a short time, formation of highly reactive ions, rapid start-up and cooling of plasma reactors.[38] To improve the efficiency of defluorination, primarily the volatile materials were released during the carbonization temperature in an inert atmosphere, which was maintained with a constant flow of argon. These chars are the product of biomass carbonization in the absence of oxygen at a very high temperature of 1600 °C in a plasma furnace. The graphite crucible containing the charge acted as the bottom electrode. The extended arc was formed by the movement of the top graphite with an axial hole through which the argon plasma forming gas was introduced. The formation of plasma occurred when the electric discharge passes through the gas, which ionised the gas molecules and generated heat due to electrical resistivity of the system.[38] For preparing the biochar under a plasma reactor, the dried materials were processed at 1600 °C for 3 min. During such reaction, the bonds of oxygen with carbon are broken, thus increasing the efficiency by exposing the adsorption site to fluoride for adsorption. The samples have very less oxygen and ash contents with a high carbon content up to 80%, which increases the efficiency of the samples due to surface adsorbate site exposed. Since a high ash content adversely affects the activated carbon as an adsorbent material, a thermal plasma route is preferred in preparing the biochar with minimal ash contents. The plasma-treated sample is black in colour and fragile in nature, and thus, it could be easily ground in a mortar and pestle. It was observed that within two minutes, the volatile was removed in a plasma furnace. The samples were synthesized by a special method and used without further treatment.

3.2 Biochar-based fluoride adsorption in synthetic water

Different parts of the plant were dried separately and taken for plasma processing to prepare biochars for fluoride removal. Proximate analysis was used to analyze the moisture content, volatile matter, fixed carbon and ash contents (Table S1†). Proximate analysis clearly indicates that the physiochemical activation successfully increased the fixed carbon content and decreased the volatile matter.[43] Though *Moringa oleifera* seed has been used for the removal of heavy metals from aqueous solutions,[44] no reports are available on the removal of fluoride using biochars of *Moringa* plant parts like the seed and leaf. Keeping this as background, the initial experiment of fluoride adsorption was conducted for 12 h with different biochar samples as the *Moringa* leaf, younger stem, bark-free younger stem, youngest stem with leaves, bark-free oldest stem, bark-free older stem, bark, and seed. The fluoride concentration in the synthetic water was kept up to 2 ppm. *Moringa* biochars adsorbed 10%, bark-free oldest stem adsorbed 17%, bark-free younger stem adsorbed 19.8%, bark-free older stem adsorbed 24%, bark adsorbed 27%, leaf biochars adsorbed 44%, younger stem adsorbed 49%, the youngest stem with leaves adsorbed 55%, while seed biochars adsorbed 100% (Fig. 1a). Interestingly, a minimal amount of fluoride was noticed with the filtrate from *Moringa* seeds. Thus, *Moringa* seed biochars are best F^- adsorbents as compared to other parts of the *Moringa oleifera* plant. The next experiment was conducted to examine how much minimum amount of biochars are required for fluoride adsorption.

3.3 Fluoride adsorption using moringa seed biochars

To study the adsorption efficiency, different percentages of *Moringa* biochars were taken for treatment of 2 ppm of fluoride for 2 h. The biochar of *Moringa* seed was weighed in a weighing balance separately as 0.0125, 0.025, 0.05, and 0.1 g and added to 10 mL water containing 2 ppm fluoride (Fig. S1†). The percentage of removal of fluoride increased by increasing the biochar concentration. The capacity of fluoride adsorption was sharply increased from 0.0125 g to 0.05 g, while 0.1 g of biochar was able to adsorb nearly 100% of fluoride. Thus, the more the amount of adsorbent available, the more the surface area for ion-exchange and adsorption. Nevertheless, 0.05 to 0.1 g of biochar is sufficient to remove fluoride completely from 10 mL of standard solution. To move further, different concentrations of fluoride solutions were examined with the fixed amount of biochars. One gram of *Moringa* seed biochars was used for 100 mL water with fluoride concentrations of 2, 4, 8 and 12 ppm. After 48 h of incubation, the removal efficiency was slightly lowered with the increase in concentration. *Moringa* seed biochars were able to remove 96%, 92%, 84% and 42% of fluoride from 2 ppm, 4 ppm, 8 ppm and 12 ppm fluoride solutions, respectively. From 2 and 4 ppm, the removal is 96%, and 92%, respectively, whereas from 8 and 12 ppm, we noticed 84% and 42% removal respectively. Possibly after increasing the fluoride concentration and keeping the adsorbant amount constant, the removal of fluoride was gradually lowered. This is due to the saturation of the active adsorbant site, and sufficient hydroxyl ions are generated due to protonation and ion exchange, which compete with the active adsorbate site in place of fluoride.

3.4 Biochar-based fluoride adsorption in ground water samples of nuapada district

To validate the fluoride removal ability of seed biochars of *Moringa oleifera*, different ground water samples were collected from Nuapada district, which were contaminated with fluoride. Five samples collected from 4 villages were labelled Sample 1 to

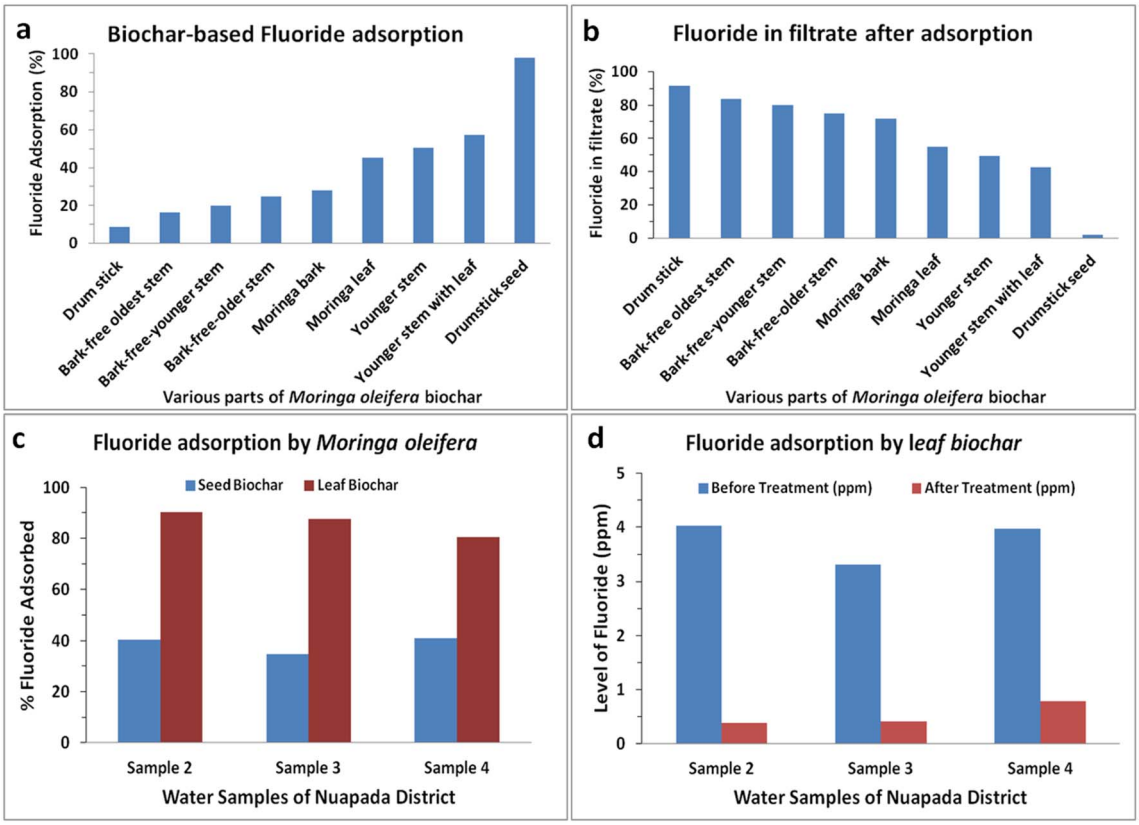

Fig. 1 Fluoride adsorption in a standard fluoride solution using biochars of different parts of *Moringa oleifera* (a). Drumstick biochar adsorbed 10%, bark-free oldest stem adsorbed 17%, bark-free younger stem adsorbed 19.8%, bark-free older stem adsorbed 24%, bark adsorbed 27%, leaf biochars adsorbed 44%, younger stem adsorbed 49%, the youngest stem with leaves adsorbed 55%, while seed biochars adsorbed 100%. The fluoride content in the filtrate after biochar-based fluoride removal (b). Removal of fluoride from contaminated ground water samples collected from Nuapada district of Odisha. Fluoride adsorbed using *Moringa oleifera* seed and leaf biochars in 18 sh (c). Level of fluoride in the groundwater samples before and after treatment with leaf biochars (d).

5, and the fluoride content ranged from 0.932 to 6.12 (Table S1†). When seed biochars were applied to different groundwater samples and incubated for 1 h, the adsorption of F^- for Sample 1 to 5 was 35%, 40%, 35%, 40%, and 60%, respectively. The variation in the pattern of adsorption is possibly due to the interfering ions present in the groundwater samples. The chemical composition on the surface of the seed biochar as well as the porosity and other physicochemical parameters might participate in the ionic interaction and other anions present in the sample most likely interfere with the process.

Since the adsorption with seed biochars was compromised with regard to the standard F^- solution, we explored other materials such as *Moringa* stems with leaves, which were next to seed biochars in adsorbing F^- from the standard solution (Fig. 1a and b). Similarly, the biochar of *Moringa* younger stems with leaves was incubated with groundwater samples for 1 h. The adsorption with stem-leaf biochars presents 25%, 80%, 65%, 60% and 55% removal (data not shown). It seems that the F^- adsorption capacity of different biochars differs and stems with leaves are better than seed biochars. Nevertheless, the removal efficiency of F^- is largely compromised with ground water due to the difference in composition as compared to the standard F^- solution. Thus, we enquired whether the biochar from leaves alone can be a better substance for F^- removal in ground water samples.

When ground water Samples 2, 3 and 4 were separately treated with seed and leaf biochars, surprisingly the removal efficiency was two times more in leaf biochars than in seed biochars (Fig. 1c). When the seed biochar was able to remove nearly 40% of F^- from Sample 2, the leaf biochar efficiently removed close to 90% of F^- in the same experimental set up. Similar findings were also observed with Samples 3 and 4. Though the removal efficiency was not similar in all water samples with the leaf biochar, but irrespective of the ground water the leaf biochar is a better candidate than the seed biochar in removing F^- (Fig. 1d). Thus, one generic biochar may not be applicable for all F^--contaminated ground water samples, and at the same time, the biochar or similar adsorbent materials that are very efficient in removing F^- from the standard solution may not suitable in real-life applications. It is imperative to understand the mechanism of differential F^- adsorption in different biochar materials.

3.5 Elemental characterization of moringa biochars

The detector allows for the detection of elements C, Ca, O, Al, Mg, and S, in leaf biochars, whereas C, O, Al, and Mg in seed

biochars (Table S2†). The carbon, oxygen, aluminium, calcium, sulphur, and magnesium content in leaf biochars was 89.45%, 12%, 18%, 4.64%, 0.50%, and 0.47%, respectively. Possibly, the positive charge on the surface of the adsorbent is due to the presence of Al, Mg, and Ca. Since the carbon content in biochars is responsible for fluoride adsorption, the sample with the highest amount of carbon is said to be the most efficient adsorbent. Magnesium, aluminium, silicon, manganese, and iron fluorides have only slight water solubilities. Nevertheless, calcium salts in the char could form insoluble fluorides. Thus, these compounds in biochars enhanced fluoride adsorption in ground water. Fluoride adsorption *via* a two-step ligand exchange was reported, where the pH of the remediated water solution increased after fluoride sorption.[45] To further understand, the biochar surface was thoroughly analyzed by SEM.

3.6 Scanning electron microscopy of biochars

The surface of the leaf biochar of *Moringa oleifera* has a higher surface area and porosity. Moreover, the EDX spectra clearly show the presence of C, Ca, Mg, and Al on the surface of biochars (Fig. 2). Nevertheless, the presence of F^- spectra in the leaf biochar after treatment supports the efficient F^- adsorption and removal from ground water (Fig. 3). The key mechanism of F^- adsorption is most probably due to the presence of Ca and C, which have strong affinity for F^-. The complex can be precipitated or immobilized as CaF_2. Moreover, the presence of calcium-containing materials such as $Ca(OH)_2$ and CaO also enhances F^- adsorption due to strong binding affinity between calcium and fluoride. FESEM data also support the generation of pores, which takes place *via* selective elimination of reactive carbon. Thus, high surface area and favourable porous architecture and carbon-rich biochars help in the adsorption of fluoride. Possibly, the seed has a lower surface area than that of the leaf (Fig. 2, S2 and S3†). The lower adsorption for groundwater samples in seed biochars is due to the ionic interference and lower carbon content. The surface morphology is an important factor in adsorbent–adsorbate interactions. The figures clearly demonstrate the porous surfaces with a disorganized structural pattern that still contains the original morphology of wood cells. The macropore size distribution has discrete groups of pore sizes rather. These pores are of importance to many liquid–solid adsorption processes. Instead, chemical decomposition has occurred with loss of water and organic fragments which reduce the total mass by at least 80%. Macropores formed on the *Moringa* seed biochar surface are coarser and rougher than those of the *Moringa* leaf char surface. The vesicles on the smooth surface of *Moringa* leaves resulted from the release of volatile gas contained in the softened biomass matrix during plasma furnace processing. Metal fluoride bonds are strong and the solubility of CaF_2 and AlF_3 in water is extremely low. Nevertheless, fluoride is known to interact with hydrous aluminium oxides and alumina;[46] thus, the presence of Al on the biochar of *Moringa oleifera* leaves supports fluoride adsorption in contaminated drinking water.

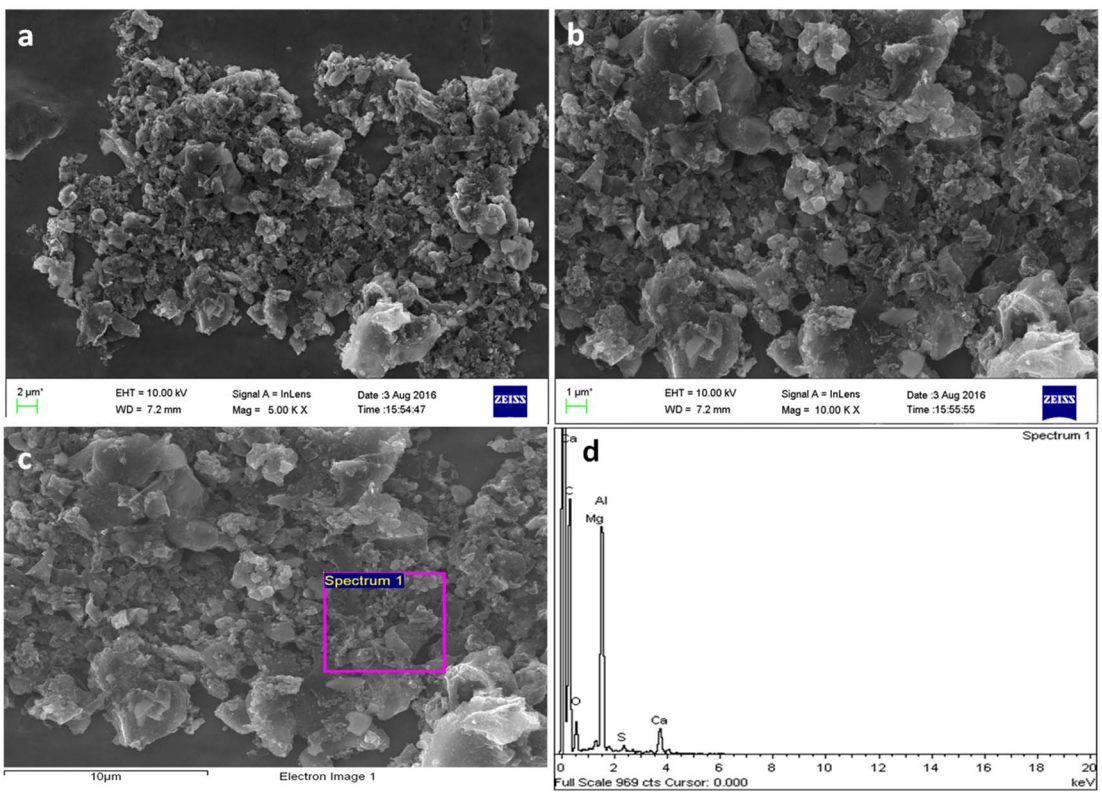

Fig. 2 FESEM images of the *Moringa* leaf biochar before fluoride adsorption. All images show a higher surface area and porosity (a, b and c). EDX spectra of the leaf biochar showing the presence of Ca, C, O, Al, Mg, and S (d).

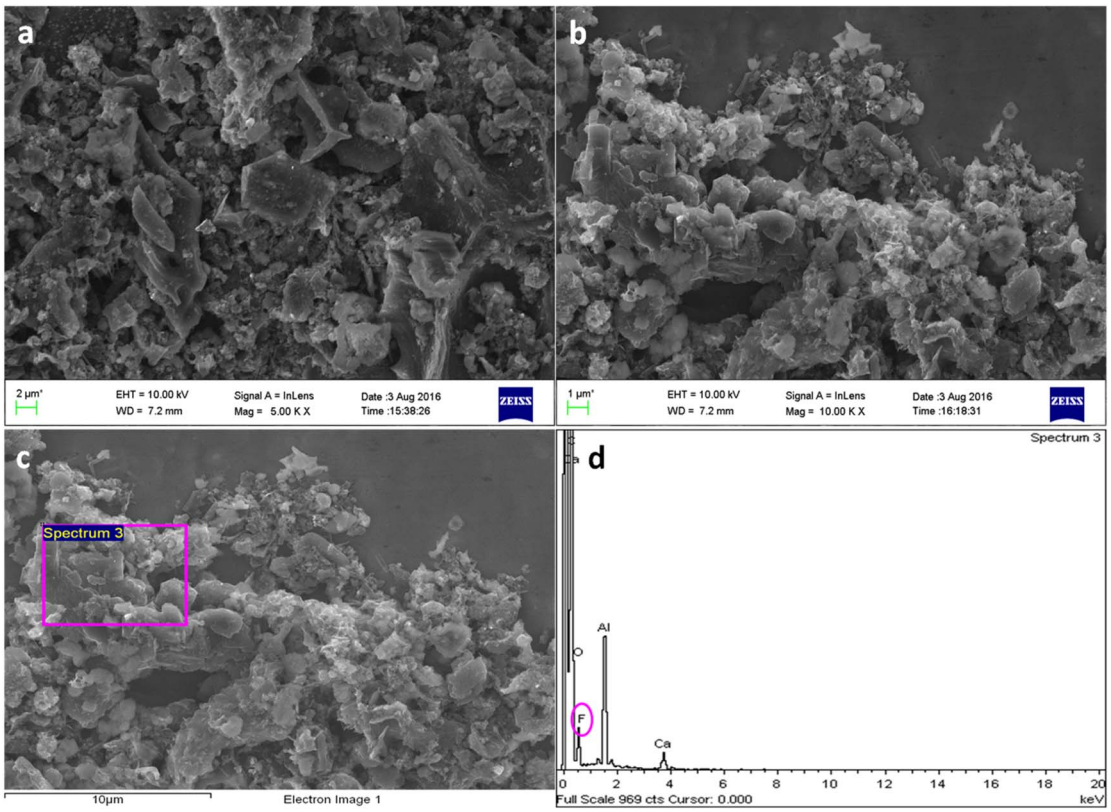

Fig. 3 FESEM images of the *Moringa* leaf biochar after fluoride adsorption (a, b and c). EDX spectra of the *Moringa* leaf biochar showing the presence of Ca, C, O, F, Al, and Mg (d).

Further, an X-ray diffraction study was carried out to examine the nature of biochar.

3.7 X-ray diffraction of biochars

The powder X-ray diffraction pattern of *Moringa* leaf biochars is represented in the black spectra, which shows the crystalline structure of CaO, KO_2, MgO, $Ca(OH)_2$, and amorphous carbons up to 80% (Fig. 4). The peak were observed at 2θ values in the (001) plane for $Ca(OH)_2$ (00-044-1481), (002) for carbon (00-026-1080), (102) for CaO (01-070-4068), (104) and (006) for KO_2 (00-039-0697), (110) for $Ca(OH)_2$ (01-089-8487), and (200) for MgO (01-075-0447) using JCPDS files. The samples represented in the red spectra (*Moringa* leaf biochars after fluoride adsorption) show two intense peaks for carbon- and oxygen-bonded

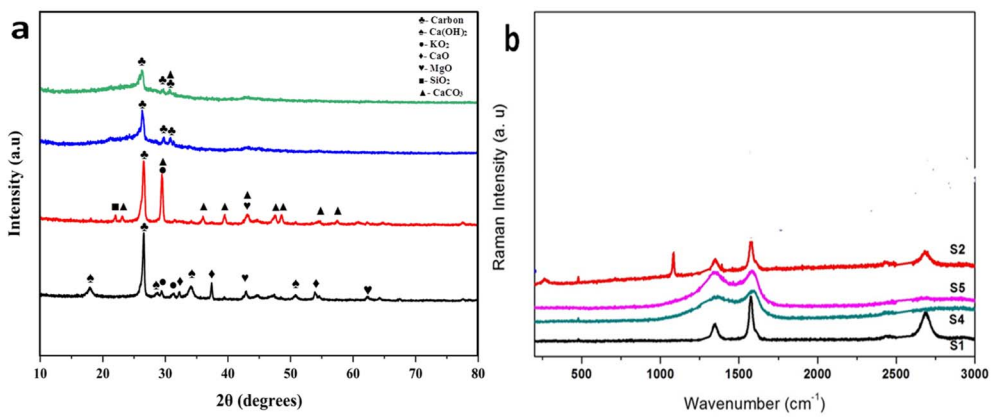

Fig. 4 XRD spectra of the leaf biochar of *Moringa oleifera* before (black spectrum) and after (red spectrum) fluoride adsorption. XRD spectra of the seed biochar of *Moringa oleifera* before (blue spectrum) and after (green spectrum) fluoride adsorption (a). RAMAN spectra of the leaf biochar of *Moringa oleifera* before (black spectrum) and after (red spectrum) fluoride adsorption. RAMAN spectra of the seed biochar of *Moringa oleifera* before (green spectrum) and after (pink spectrum) fluoride adsorption (b).

functional groups such as $CaCO_3$, and smaller peaks for SiO_2, KO_2, and MgO. Other peaks are not observed due to adsorption of fluoride, which has affinity for calcium that results in distorted structures of CaO and $Ca(OH)_2$ crystals due to new bond formation between calcium and fluorine atoms. The 2θ values in the planes (012), (104), (110), (113) (202) (018) (116), and (122) for $CaCO_3$ and (100) for SiO_2 were also observed. The spectrum of seed biochars (blue line) shows peak only for carbon but devoid of Ca. The green line stands for the seed biochar after fluoride adsorption, which also shows the peak of carbon and $CaCO_3$. This means the crystal structure is distorted after fluoride adsorption and no more crystal phase is visible. The crystallite size was determined using Scherrer's formula: $D = \frac{0.9\lambda}{\beta \cos \theta}$, where D is the crystallite size, λ is the wavelength of radiation, β is the full width at half maximum of the peak and θ is Bragg's angle. The crystallite size of some structures such as $Ca(OH)_2$, KO_2, MgO, CaO, $CaCO_3$, SiO_2, and C were 20.94, 25.78, 44.46, 74.90, 25.94, 34.52, and 39.24 nm, respectively. The average crystallite size of the biochar presented in the black, red, blue and green spectra was found to be 32.68, 32.88, 29.34 and 58.01 nm, respectively. Interestingly, the crystallite size remained unaltered in the leaf biochar during defluoridation, while the crystallite size became double for the seed biochar. To examine further, the Raman spectra were analysed for the seed and leaf biochars.

3.8 Raman study of biochars

The biochars contain substantial oxygen (8–11%) throughout the solid enhancing hydrophilicity. The Raman spectra of these biochars display bands due to different oxygen-containing functional groups (C═O, C–O, and –OH). Oxygen-containing functional groups can serve as potential sites for adsorption and assist in water penetration and swelling of biochar solids. Activated carbon contains macropores close to the surface that branch into mesopores and finally micropores. Macropores represent the entrance to the internal adsorbent pore structure, and mesopores facilitate diffusive transport to adsorption sites in the micropores. S2 represents the used biochar after 18 h of fluoride adsorption, which shows a peak at 1400 cm^{-1}, a sharp peak at 1600 cm^{-1} and between 2600 and 2800 cm^{-1}. Peak between 1000 to 1400 cm^{-1} is assigned for C–O, and C–N, 1400 to 1600 cm^{-1} represents for C═C, C–N. 2600 to 2800 cm^{-1} corresponds to C–H, O═C–H. The peak near 1580 cm^{-1} represents the G-band due to bond stretching of all pairs of the SP2 atom and 1350 cm^{-1} represents the D-peak due to the breathing mode of SP2 (Fig. 4).[47] Thus, we can conclude the bonds noticed in the used biochar; bonds below 650 cm^{-1} is for C–F, C–Br, and C–I. While 3700–2500 cm^{-1} represents single bonds to hydrogen, 2300–2000 cm^{-1} for triple bonds, 1900–1500 cm^{-1} is for double bonds, 1400–650 cm^{-1} for single bond (other than hydrogen), between 3000 to 2800 cm^{-1} represents C–H bonds, between 200 to 1500 cm^{-1} for C═O, C═N. The expected functional groups are aldehyde, esters, ketones, carboxylic acid, amines, and weak C═C bonds. The peaks obtained for Sample 1 show the presence of C–O, C–N, C–C, C–H, O═C–H, and C–F. The peaks obtained for Sample 2 showed C–F, C–O, C–N, C═C, and weak bonds of C–H. Thus, the presence of carbonyl, sulfhydryl, thioether, amine, amide bonds, *etc.*, on the biosorbent was confirmed. All these bonds along with the metal ions and high porosity of carbon are responsible for biosorption of fluoride selectively. We can say that other ions present in the groundwater sample may interfere with the process, but still the activated *Moringa* leaf sample is efficient enough to adsorb up to 85% fluoride from the sample.

3.9 Effect of biochars on the growth of microbes in a nutrient broth

Three different concentrations of *Moringa oleifera* biochars were used to study the antibacterial activity on *E. coli* following the procedure reported earlier.[48] Based on 6 h time interval, three

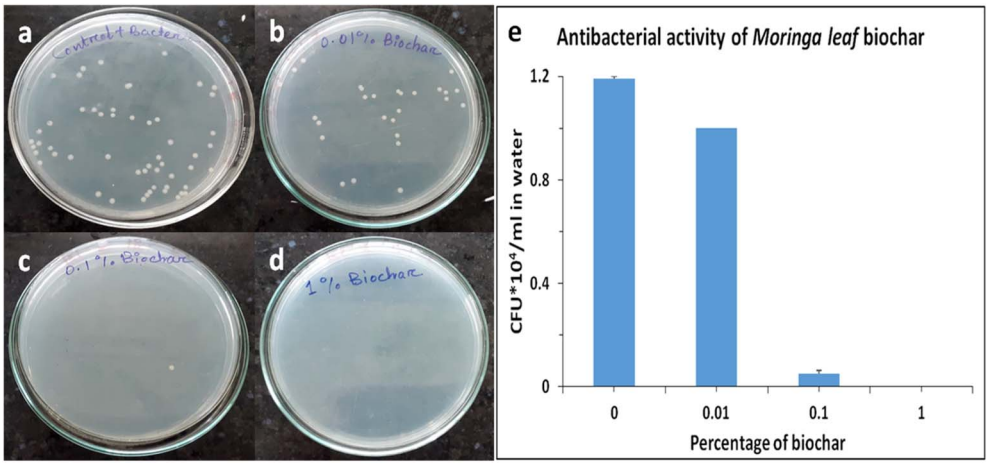

Fig. 5 Antibacterial activity of the *Moringa oleifera* biochar on *Escherichia coli*. Pure cultures of *E. coli* were mixed with autoclaved MQ water in the presence of different concentrations of leaf biochars, 0%, 0.01%, 0.1%, and 1%. After 6 h of incubation, suitably diluted samples were spread into LB agar plates (a) 0%, (b) 0.01%, (c) 0.1% and (d) 1%. The disappearance of colonies with the increase in concentrations of biochar implies the antibacterial activity of *Moringa* biochars (e).

distinctly different and descending growth rates were observed as compared to the biochar-free control growth rate. The decay rate increased substantially, with the increase in biochar concentration, as indicated by the disappearance of CFU in 1% leaf biochar. Bacterial inhibition was calculated using the formula log reduction $= \log_{10}(N_t/N_0)$, where N_0 is the colony count of water sample before experimentation at time $t = 0$ and N_t is the colony count of water sample after experimentation at time t.

The trends of bacterial growth in the presence of different concentrations of biochars in the nutrient medium are shown in Fig. 5. The results indicated a tendency of diminished growth with the increase in concentrations of leaf biochars. For the same initial bacterial concentration, bacterial growth was found to be 4.84×10^8 CFU mL^{-1} in control, whereas an increased biochar concentration resulted in a significant reduction in bacterial growth. A significant decrease in growth (CFU mL^{-1}) was observed for 10 mL broth containing 0.01% and 0.1% leaf biochar. It is interesting to note that the highest deterioration of growth was observed in 10 mL broth containing 1% leaf biochar. Though biochars of *Camellia oleifera* seed shell and corn stalk were explored for fluoride adsorption,[49,50] few reports demonstrate the antibacterial activity of biochars. To our knowledge, this is the first report on both defluoridation and antibacterial activities of biochars prepared from *Moringa oleifera* leaves *via* thermal plasma processing.

4. Conclusions

Biosorption is preferred over other chemically available procedures for fluoride removal because of simple design, ease of operation, non-toxicity, and economic values. The present work deals with a case study of Nuapada district of Odisha, India, where a large number of school children, young, adult, and old people are affected with dental and skeletal fluorosis because of fluoride contamination of ground water. For the removal of fluoride from the contaminated ground water, thermal plasma-based biochars were explored and it was found that the *Moringa* leaf biochar can remove > 80% of fluoride with overnight incubation. The relative contributions of the functional groups present on the biochar surface depends on the sample processing of biochars and also the raw materials. We found that the seed biochar which was efficient in fluoride adsorption in a standard Fluoride solution is very poor in ground water, whereas the leaf biochar which was a poor adsorbent for a standard F^- solution is a potential candidate for F^- adsorption in ground water. Thus, a series of biochars need to be identified for different locations and depending upon the nature of contamination. One generic biochar may not be applicable for all contaminants or fluoride removal from all the contaminate sources. The preliminary results of thermal plasma processing motivate to scale up the process and also search for other possible materials suitable for the removal of fluoride or any such metal contaminates from water. This is the first report to highlight the fluoride removal from ground water using biochars and it was noticed that the composition of different ground water samples is different, and hence, a thorough study is required to come-up with a site-specific solution for such unique problems.

Conflicts of interest

The authors declare that they have no known competing financial interests or personal relationships that could have appeared to influence the work reported in this paper.

Acknowledgements

Authors are thankful to the Council of Scientific and Industrial Research (CSIR), Government of India, New Delhi for financial assistance.

References

1 I. Hussain, M. Arif and J. Hussain, Fluoride contamination in drinking water in rural habitations of Central Rajasthan, India, *Environ. Monit. Assess.*, 2012, **184**, 5151–5158, DOI: 10.1007/s10661-011-2329-7.
2 D. Saralakumari and P. R. Rao, Endemic fluorosis in the village Ralla Anantapuram in Andhra Pradesh: An epidemiological study, *Fluoride – Q. Rep.*, 1993, **26**, 177–180.
3 A. Chowdhury, M. K. Adak, A. Mukherjee, P. Dhak, J. Khatun and D. Dhak, A critical review on geochemical and geological aspects of fluoride belts, fluorosis and natural materials and other sources for alternatives to fluoride exposure, *J. Hydrol.*, 2019, **574**, 333–359, DOI: 10.1016/j.jhydrol.2019.04.033.
4 M. Amini, K. Mueller, K. C. Abbaspour, T. Rosenberg, M. Afyuni, K. N. Møller, M. Sarr and C. A. Johnson, Statistical modeling of global geogenic fluoride contamination in groundwaters, *Environ. Sci. Technol.*, 2008, **42**(10), 3662–3668, DOI: 10.1021/es071958y.
5 D. Banks, C. Reimann, O. Røyset, H. Skarphagen and O. M. Sæther, Natural concentrations of major and trace elements in some Norwegian bedrock groundwaters, *Appl. Geochem.*, 1995, **10**(1), 1–16, DOI: 10.1016/0883-2927(94)00046-9.
6 P. T. C. Harrison, Fluoride in water: A UK perspective, *J. Fluorine Chem.*, 2005, **126**(11–12), 1448–1456, DOI: 10.1016/j.jfluchem.2005.09.009.
7 S. Ayoob and A. K. Gupta, Fluoride in drinking water: A review on the status and stress effects, *Crit. Rev. Environ. Sci. Technol.*, 2006, **36**(6), 433–487, DOI: 10.1080/10643380600678112.
8 N. Dash, S. P. Das, T. Patnaik, S. B. Patel and R. K. Dey, Fluoride concentration in groundwater of Kalahandi and Nuapada District, Odisha, India, *Der Chemica Sinica*, 2015, vol. 6.
9 M. K. Mahapatra, A. Mishra and B. P. Das, Fluorosis 1st Reported in Nuapada District of Orissa, India, *Ecol., Environ. Conserv.*, 2005, **11**, 277–280.
10 E. J. Reardon and Y. Wang, A limestone reactor for fluoride removal from wastewaters, *Environ. Sci. Technol.*, 2000, **34**(15), 3247–3253, DOI: 10.1021/es990542k.

11 Y. Zhou, C. Yu and Y. Shan, Adsorption of fluoride from aqueous solution on La3+-impregnated cross-linked gelatin, *Sep. Purif. Technol.*, 2004, **36**(2), 89–94, DOI: 10.1016/S1383-5866(03)00167-9.

12 M. Islam and R. Patel, Thermal activation of basic oxygen furnace slag and evaluation of its fluoride removal efficiency, *Chem. Eng. J.*, 2011, **169**(1–3), 68–77, DOI: 10.1016/j.cej.2011.02.054.

13 A. Bhatnagar, E. Kumar and M. Sillanpää, Fluoride removal from water by adsorption-A review, *Chem. Eng. J.*, 2011, **171**(3), 811–840, DOI: 10.1016/j.cej.2011.05.028.

14 A. Mukherjee, M. K. Adak, S. Upadhyay, J. Khatun, P. Dhak, S. Khawas, U. K. Ghorai and D. Dhak, Efficient Fluoride Removal and Dye Degradation of Contaminated Water Using Fe/Al/Ti Oxide Nanocomposite, *ACS Omega*, 2019, **4**(6), 9686–9696, DOI: 10.1021/acsomega.9b00252.

15 M. K. Adak, A. Sen, A. Mukherjee, S. Sen and D. Dhak, Removal of fluoride from drinking water using highly efficient nano-adsorbent, Al(III)-Fe(III)-La(III) trimetallic oxide prepared by chemical route, *J. Alloys Compd.*, 2017, **719**, 460–469, DOI: 10.1016/j.jallcom.2017.05.149.

16 O. Ekpete, M. Horsfall Jnr and T. Tarawou, Evaluation of Activated Carbon from Fluted Pumpkin Stem Waste for Phenol and Chlorophenol Adsorption in a Fixed –Bed Micro-Column, *J. Appl. Sci. Environ. Manage.*, 2011, **15**, DOI: 10.4314/jasem.v15i1.65691.

17 E. Pehlivan, H. Kahraman and E. Pehlivan, Sorption equilibrium of Cr(VI) ions on oak wood charcoal (Carbo Ligni) and charcoal ash as low-cost adsorbents, *Fuel Process. Technol.*, 2011, **92**(1), 65–70, DOI: 10.1016/j.fuproc.2010.08.021.

18 F. Y. Wang, H. Wang and J. W. Ma, Adsorption of cadmium (II) ions from aqueous solution by a new low-cost adsorbent-Bamboo charcoal, *J. Hazard. Mater.*, 2010, **177**(1–3), 300–306, DOI: 10.1016/j.jhazmat.2009.12.032.

19 H. Wei, S. Deng, B. Hu, Z. Chen, B. Wang, J. Huang and G. Yu, Granular bamboo-derived activated carbon for high CO_2 adsorption: The dominant role of narrow micropores, *ChemSusChem*, 2012, **5**(12), 2354–2360, DOI: 10.1002/cssc.201200570.

20 T. S. Anirudhan and S. S. Sreekumari, Adsorptive removal of heavy metal ions from industrial effluents using activated carbon derived from waste coconut buttons, *J. Environ. Sci.*, 2011, **23**(12), 1989–1998, DOI: 10.1016/S1001-0742(10)60515-3.

21 M. A Hashem, Adsorption of lead ions from aqueous solution by okra wastes, *Int. J. Phys. Sci.*, 2007, **2**, 178–184.

22 N. T. Abdel-Ghani, M. Hefny and G. A. F. El-Chaghaby, Removal of lead from aqueous solution using low cost abundantly available adsorbents, *Int. J. Environ. Sci. Technol.*, 2007, **4**, 67–73, DOI: 10.1007/BF03325963.

23 N. Meunier, J. Laroulandie, J. F. Blais and R. D. Tyagi, Cocoa shells for heavy metal removal from acidic solutions, *Bioresour. Technol.*, 2003, **90**(3), 255–263, DOI: 10.1016/S0960-8524(03)00129-9.

24 B. J. Mcafee, W. D. Gould, J. C. Nadeau and A. C. A. Da Costa, Biosorption of metal ions using chitosan, chitin, and biomass of Rhizopus oryzae, *Sep. Sci. Technol.*, 2001, **36**(14), 3207–3222, DOI: 10.1081/SS-100107768.

25 D. Mohan, C. U. Pittman, M. Bricka, F. Smith, B. Yancey, J. Mohammad, P. H. Steele, M. F. Alexandre-Franco, V. Gómez-Serrano and H. Gong, Sorption of arsenic, cadmium, and lead by chars produced from fast pyrolysis of wood and bark during bio-oil production, *J. Colloid Interface Sci.*, 2007, **310**(1), 57–73, DOI: 10.1016/j.jcis.2007.01.020.

26 B. Yu, Y. Zhang, A. Shukla, S. S. Shukla and K. L. Dorris, The removal of heavy metals from aqueous solutions by sawdust adsorption – Removal of lead and comparison of its adsorption with copper, *J. Hazard. Mater.*, 2001, **84**(1), 83–94, DOI: 10.1016/S0304-3894(01)00198-4.

27 S. Gueu, B. Yao, K. Adouby and G. Ado, Kinetics and thermodynamics study of lead adsorption on to activated carbons from coconut and seed hull of the palm tree, *Int. J. Environ. Sci. Technol.*, 2007, **4**, 11–17, DOI: 10.1007/BF03325956.

28 S. K. R. Yadanaparthi, D. Graybill and R. von Wandruszka, Adsorbents for the removal of arsenic, cadmium, and lead from contaminated waters, *J. Hazard. Mater.*, 2009, **171**(1–3), 1–15, DOI: 10.1016/j.jhazmat.2009.05.103.

29 D. Mohan, R. Sharma, V. K. Singh, P. Steele and C. U. Pittman, Fluoride removal from water using bio-char, a green waste, low-cost adsorbent: Equilibrium uptake and sorption dynamics modeling, *Ind. Eng. Chem. Res.*, 2012, **51**(2), 900–914, DOI: 10.1021/ie202189v.

30 L. Li, P. A. Quinlivan and D. R. U. Knappe, Effects of activated carbon surface chemistry and pore structure on the adsorption of organic contaminants from aqueous solution, *Carbon N. Y.*, 2002, **40**(12), 2085–2100, DOI: 10.1016/S0008-6223(02)00069-6.

31 A. Demirbas, Heavy metal adsorption onto agro-based waste materials: A review, *J. Hazard. Mater.*, 2008, **157**(2–3), 220–229, DOI: 10.1016/j.jhazmat.2008.01.024.

32 A. N. A. El-Hendawy, Surface and adsorptive properties of carbons prepared from biomass, *Appl. Surf. Sci.*, 2005, **252**(2), 287–295, DOI: 10.1016/j.apsusc.2004.11.092.

33 X. Fan, D. J. Parker and M. D. Smith, Adsorption kinetics of fluoride on low cost materials, *Water Res.*, 2003, **37**(20), 4929–4937, DOI: 10.1016/j.watres.2003.08.014.

34 D. Mohan, S. Rajput, V. K. Singh, P. H. Steele and C. U. Pittman, Modeling and evaluation of chromium remediation from water using low cost bio-char, a green adsorbent, *J. Hazard. Mater.*, 2011, **188**(1–3), 319–333, DOI: 10.1016/j.jhazmat.2011.01.127.

35 D. Mohan, A. Sarswat, Y. S. Ok and C. U. Pittman, Organic and inorganic contaminants removal from water with biochar, a renewable, low cost and sustainable adsorbent - A critical review, *Bioresour. Technol.*, 2014, **160**, 191–202, DOI: 10.1016/j.biortech.2014.01.120.

36 C. Padilla, N. Valenciaga, G. Crespo, D. González and I. Garcia, Agronomical requirements of moringa oleifera (Lam.) in livestock systems, *Livest. Res. Rural. Dev.*, 2017, **29**, 218.

37 P. G. Milla, R. Penalver and G. Nieto, Health Benefits of Uses and Applications of Moringa oleifera in Bakery Products, *Plants*, 2021, **10**(2), 318, DOI: **10.3390/plants10020318**.

38 S. K. Singh, B. C. Mohanty and S. Basu, Synthesis of SiC from rice husk in a plasma reactor, *Bull. Mater. Sci.*, 2002, **25**, 561–563, DOI: **10.1007/BF02710551**.

39 M. A. Ahmad and R. Alrozi, Optimization of preparation conditions for mangosteen peel-based activated carbons for the removal of Remazol Brilliant Blue R using response surface methodology, *Chem. Eng. J.*, 2010, **165**(3), 883–890, DOI: **10.1016/j.cej.2010.10.049**.

40 J. Panigrahi, D. Behera, I. Mohanty, U. Subudhi, B. B. Nayak and B. S. Acharya, Radio frequency plasma enhanced chemical vapor based ZnO thin film deposition on glass substrate: A novel approach towards antibacterial agent, *Appl. Surf. Sci.*, 2011, **258**(1), 304–311, DOI: **10.1016/j.apsusc.2011.08.056**.

41 S. Majumder, M. Priyadarshini, U. Subudhi, G. B. N. Chainy and S. Varma, X-ray photoelectron spectroscopic investigations of modifications in plasmid DNA after interaction with Hg nanoparticles, *Appl. Surf. Sci.*, 2009, **256**(2), 438–442, DOI: **10.1016/j.apsusc.2009.06.097**.

42 I. Abe, S. Iwasaki, T. Tokimoto, N. Kawasaki, T. Nakamura and S. Tanada, Adsorption of fluoride ions onto carbonaceous materials, *J. Colloid Interface Sci.*, 2004, **275**(1), 35–39, DOI: **10.1016/j.jcis.2003.12.031**.

43 K. A. Adegoke and O. S. Bello, Dye sequestration using agricultural wastes as adsorbents, *Water Resour. Ind.*, 2015, **12**, 8–24, DOI: **10.1016/j.wri.2015.09.002**.

44 V. Obuseng, F. Nareetsile and H. M. Kwaambwa, A study of the removal of heavy metals from aqueous solutions by Moringa oleifera seeds and amine-based ligand 1,4-bis [N,N-bis(2-picoyl)amino]butane, *Anal. Chim. Acta*, 2012, **730**, 87–92, DOI: **10.1016/j.aca.2012.01.054**.

45 A. A. M. Daifullah, S. M. Yakout and S. A. Elreefy, Adsorption of fluoride in aqueous solutions using KMnO4-modified activated carbon derived from steam pyrolysis of rice straw, *J. Hazard. Mater.*, 2007, **147**(1–2), 633–643, DOI: **10.1016/j.jhazmat.2007.01.062**.

46 H. Farrah, J. Slavek and W. F. Pickering, Fluoride interactions with hydrous aluminium oxides and alumina, *Aust. J. Soil Res.*, 1987, **25**(1), 55–69, DOI: **10.1071/SR9870055**.

47 A. Mukherjee, N. Goswami and D. Dhak, Photocatalytic Remediation of Industrial Dye Waste Streams Using Biochar and Metal-Biochar Hybrids: A Critical Review, *Chem. Afr.*, 2022, DOI: **10.1007/s42250-022-00467-5**.

48 N. Biswal, S. Martha, U. Subudhi and K. M. Parida, Incorporation of silver ions into Zirconium Titanium Phosphate: A Novel Approach towards Antibacterial Activity, *Ind. Eng. Chem. Res.*, 2011, **50**(16), DOI: **10.1021/ie102199b**.

49 L. Mei, H. Qiao, F. Ke, C. Peng, R. Hou, X. Wan and H. Cai, One-step synthesis of zirconium dioxide-biochar derived from Camellia oleifera seed shell with enhanced removal capacity for fluoride from water, *Appl. Surf. Sci.*, 2020, **509**, 144685, DOI: **10.1016/j.apsusc.2019.144685**.

50 X. Zhang, Y. Qi, Z. Chen, N. Song, X. Li, D. Ren and S. Zhang, Evaluation of fluoride and cadmium adsorption modification of corn stalk by aluminum trichloride, *Appl. Surf. Sci.*, 2021, **543**, 148727, DOI: **10.1016/j.apsusc.2020.148727**.